The Astrophysical Journal Letters, 822:L6 (5pp), 2016 May 1 doi:10.3847/2041-8205/822/1/L6

BENCHMARK TRANSITING BROWN DWARF LHS 6343 C: *SPITZER* SECONDARY ECLIPSE OBSERVATIONS YIELD BRIGHTNESS TEMPERATURE AND MID-T SPECTRAL CLASS

Benjamin T. Montet[1,2], John Asher Johnson[2], Jonathan J. Fortney[3], and Jean-Michel Desert[4]
[1] Cahill Center for Astronomy and Astrophysics, California Institute of Technology, 1200 E. California Blvd., MC 249-17, Pasadena, CA 91106, USA; btm@astro.caltech.edu
[2] Harvard-Smithsonian Center for Astrophysics, 60 Garden Street, Cambridge, MA 02138, USA
[3] Department of Astronomy and Astrophysics, University of California, Santa Cruz, CA 95064, USA
[4] Anton Pannenkoek Astronomical Institute, University of Amsterdam, 1090 GE Amsterdam, The Netherlands
Received 2016 January 2; revised 2016 March 28; accepted 2016 March 29; published 2016 April 22

ABSTRACT

There are no field brown dwarf analogs with measured masses, radii, and luminosities, precluding our ability to connect the population of transiting brown dwarfs with measurable masses and radii and field brown dwarfs with measurable luminosities and atmospheric properties. LHS 6343 C, a weakly irradiated brown dwarf transiting one member of an M+M binary in the *Kepler* field, provides the first opportunity to probe the atmosphere of a non-inflated brown dwarf with a measured mass and radius. Here, we analyze four *Spitzer* observations of secondary eclipses of LHS 6343 C behind LHS 6343 A. Jointly fitting the eclipses with a Gaussian process noise model of the instrumental systematics, we measure eclipse depths of 1.06 ± 0.21 ppt at 3.6 μm and 2.09 ± 0.08 ppt at 4.5 μm, corresponding to brightness temperatures of 1026 ± 57 K and 1249 ± 36 K, respectively. We then apply brown dwarf evolutionary models to infer a bolometric luminosity $\log(L_\star/L_\odot) = -5.16 \pm 0.04$. Given the known physical properties of the brown dwarf and the two M dwarfs in the LHS 6343 system, these depths are consistent with models of a 1100 K T dwarf at an age of 5 Gyr and empirical observations of field T5-6 dwarfs with temperatures of 1070 ± 130 K. We investigate the possibility that the orbit of LHS 6343 C has been altered by the Kozai–Lidov mechanism and propose additional astrometric or Rossiter–McLaughlin measurements of the system to probe the dynamical history of the system.

Key words: binaries: eclipsing – brown dwarfs – stars: late-type – stars: low-mass

1. INTRODUCTION

There are only eleven brown dwarfs with measured masses and radii (Montet et al. 2015 hereafter M15, and references therein). These objects serve as useful benchmark stars to compare theoretical predictions of physical parameters for the thousands of known brown dwarfs with measured luminosities, colors, or other atmospheric parameters (Faherty et al. 2013; Mace et al. 2013; Helling & Casewell 2014). Such comparisons are not currently possible as the only brown dwarfs with measured masses and radii and inferred atmospheric parameters are larger than field objects due to youth or irradiation and therefore not representative of their old, isolated counterparts (Stassun et al. 2006; Siverd et al. 2012).

Recently, M15 announced refined physical properties of the brown dwarf LHS 6343 C (Johnson et al. 2011), measuring a mass of $62.1 \pm 1.2\ M_{\rm Jup}$ and a radius of $0.783 \pm 0.011\ R_{\rm Jup}$. These authors also detected a secondary eclipse in the *Kepler* data set with a depth of 25 ± 7 ppm. This 3.6σ detection is insufficient for atmospheric characterization, but it allows for the possibility of observations at other wavelengths to probe the temperature, age, and atmospheric properties of the brown dwarf. LHS 6343 C presents the first opportunity to robustly measure the atmospheric properties of an old, non-inflated brown dwarf with a known mass and radius, enabling a key connection between the field and transiting brown dwarf populations.

Spitzer (Werner et al. 2004) enables observations of the secondary eclipse of LHS 6343 C behind LHS 6343 A, providing an opportunity to measure the emitted near-IR radiation from the brown dwarf. Given the low level of irradiation from the host star, LHS 6343 C should behave like a field brown dwarf for which direct mass and radius measurements are generally unobtainable (Section 5.1)

In this paper, we present detections of the secondary eclipse of LHS 6343 C in both *Spitzer* IRAC bandpasses. We measure the eclipse depths by jointly fitting a Gaussian process (GP) model to the instrumental systematics and a physical model of the astrophysical signal. We use these data to infer a temperature and age of the system through theoretical models of brown dwarf evolution, making LHS 6343 C the first non-inflated brown dwarf with a known mass, radius, and direct measurement of its atmospheric properties.

2. DATA COLLECTION AND ANALYSIS

We collected data during four separate eclipses with *Spitzer*, two each in the 3.6 and 4.5 μm IRAC bands (Fazio et al. 2004). These data were collected on 2014 July 06, July 19, September 21, and October 16 as part of the *Spitzer* Cycle 10 program 10122 (PI Montet). Data in both bandpasses were collected in subarray mode with 2.0 s exposures. In all observations, a 30 minute peak-up preceded the science observations to place the star on the detector "sweet-spot" to minimize pixel-phase effects (e.g., Ballard et al. 2010). Each set of science observations contains a total of 8768 frames spread over 4.9 hr approximately centered on the time of eclipse. For computational feasibility, we binned the observations by a factor of eight, giving a cadence of $\approx$16 s per binned data point, shorter than any astrophysical quantity of interest.

We measure the observed flux in each binned frame by performing aperture photometry, repeating this procedure 11 times with circular apertures between 1.6 and 3.5 pixels. By fitting a two-dimensional Gaussian to the 5×5 region of the

detector directly surrounding the brightest pixel, we measure the position of the star on the detector in each frame (Agol et al. 2010). We find a scatter of ∼0.1 pixels during each observation. A background estimate is calculated by fitting a Gaussian to the histogram of flux values obtained over each full frame.

2.1. Noise Model

The *Spitzer* light curves are dominated by instrumental systematics largely caused by intrapixel variability in the sensitivity of the InSb detector (Charbonneau et al. 2005; Knutson et al. 2008). To account for these systematics, we fit an instrumental model simultaneously with our secondary eclipse model. Our instrumental model is the GP model of Evans et al. (2015), who employ a covariance kernel which is a function of the centroid *xy* coordinates of the star and the time *t* of the observation. For any two points *i* and *j*, their covariance is defined such that

$$K_{ij} = k_{xy} + k_t, \tag{1}$$

where

$$k_{xy} = A_{xy}^2 \exp\left[-\left(\frac{x_i - x_j}{L_x}\right)^2 - \left(\frac{y_i - y_j}{L_y}\right)^2\right] \tag{2}$$

and

$$k_t = A_t^2\left[1 + \frac{t_i - t_j}{L_t}\sqrt{3}\right]\exp\left[-\left(\frac{t_i - t_j}{L_t}\right)\sqrt{3}\right]. \tag{3}$$

Here, x_i and y_i are the centroid positions of the star during the *i*th observation, taken at time t_i. A_{xy} and A_t define the magnitude of the correlation between data points and L_x, L_y, and L_t define the length scales of said correlation. A larger value of K_{ij}, when the temporal or spatial separation between two points is small relative to L_t, L_x, or L_y, implies a stronger correlation.

Our noise model then has 19 free parameters. As each observation falls on a different region of the detector, A_{xy}, A_t, L_x, and L_y are not shared between observations. L_t is shared between observations. We also fit for two white noise parameters, one for each bandpass, added in quadrature to our covariance kernels.

2.2. Physical Model

Simultaneously we fit a physical model of the secondary eclipses of LHS 6343 C behind LHS 6343 A. We use the transit model of Mandel & Agol (2002) with no limb darkening, as the primary star is not being occulted: the observed flux should be unchanging between second and third contact. We fit for four separate eclipse depths, allowing for the possibility of variability similar to that observed in *Spitzer* surveys of field brown dwarfs (Buenzli et al. 2012; Metchev et al. 2015). We also fit the orbital period, radius ratio between LHS 6343 A and LHS 6343 C, time of transit, eccentricity vectors $\sqrt{e}\cos\omega$ and $\sqrt{e}\sin\omega$, reduced semimajor axis $a/R_\star$, and impact parameter. For each of these, we apply a prior following the results of the simultaneous RV and transit fit of M15. With 11 parameters defining the astrophysical model, we have 30 parameters total. Our model is shown in Figure 1.

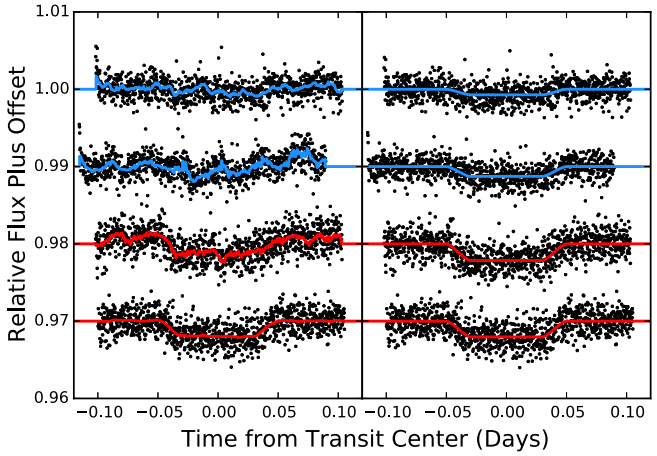

Figure 1. (Left) Observed secondary eclipses of LHS 6343 C. The solid line represents the maximum likelihood joint fit of the instrumental and astrophysical models. The observations are arranged chronologically from top to bottom. The top two, in blue, are eclipses in the IRAC 1 3.6 μm bandpass. The bottom two, in red, are taken in the IRAC 2 4.5 μm bandpass. (Right) The same eclipses, with the maximum likelihood instrumental model divided out for illustration.

2.3. Parameter Estimation

We first calculate a maximum likelihood solution for each eclipse with each of our 11 apertures. We then choose the single aperture that maximizes our likelihood function and restrict ourselves to that aperture. For the first 3.6 μm eclipse and both 4.5 μm eclipses, we find the likelihood function is maximized with a 2.0 pixel aperture; for the other 3.6 μm eclipse, we use a 2.3 pixel aperture. In all cases, these apertures include both M dwarfs in the system. To compute the covariance matrix and likelihood function for each model, we use `george`[5], an implementation of the hierarchically off-diagonal low-rank matrix solver of Ambikasaran et al. (2014).

To infer the eclipse depths, we then explore the parameter space using `emcee` (Foreman-Mackey et al. 2013), an implementation of the affine-invariant ensemble sampler of Goodman & Weare (2010). We initialize 200 walkers clustered around the maximum likelihood values for each eclipse. We then allow these walkers to evolve for 1500 steps, limiting each noise parameter to values within a factor of e^{10} of the maximum likelihood value. We remove the first 600 steps as burn-in and verify our system has converged through the test of Geweke (1992) and visual inspection.

3. RESULTS

Our results are shown in Table 1. We find less correlated noise in the 4.5 μm bandpass, in line with previous *Spitzer* analyses (Hora et al. 2008). We do not find significant evidence for variability between eclipses. In the 3.6 μm bandpass the two depths are consistent at 1.4σ; at 4.5 μm, 0.8σ. We consider these observations to represent the system in similar states and combine the likelihoods on the eclipse depth through a kernel density estimation of each individual depth. From this, we measure an eclipse depth of 1.06 ± 0.21 parts per thousand (ppt) at 3.6 μm and 2.09 ± 0.08 ppt at 4.5 μm, as shown in Figure 2. We also calculate brightness temperatures for each bandpass using the BT-Settl model spectra of Allard et al.

[5] http://dan.iel.fm/george

Table 1
Parameters for AB

Parameter	Median		Uncertainty (1σ)
IRAC 1 Parameters			
Transit Depth, 2014 Jul 06 (ppt)	0.74	±	0.27
Transit Depth, 2014 Jul 19 (ppt)	1.26	±	0.24
Transit Depth, Combined (ppt)	1.06	±	0.21
M_A (Vega)[a]	6.56	±	0.08
M_B (Vega)[a]	6.97	±	0.10
M_C (Vega)	13.43	±	0.23
T_b (K)	1026	±	57
IRAC 2 Parameters			
Transit Depth, 2014 Sep 21 (ppt)	2.16	±	0.12
Transit Depth, 2014 Oct 16 (ppt)	2.03	±	0.12
Transit Depth, Combined (ppt)	2.09	±	0.08
M_A (Vega)[a]	6.45	±	0.07
M_B (Vega)[a]	6.86	±	0.09
M_C (Vega)	12.58	±	0.07
T_b (K)	1249	±	36
System Parameters			
Time of Secondary Eclipse (BJD—2400000)	56845.401	±	0.001
Orbital Period (days)[b]	12.7137941	±	0.0000002
Eccentricity Vector $e\cos\omega$	0.0229	±	0.0001
Star C Surface Gravity (m s^{-2})[b]	2630	±	50
Star C Luminosity ($\log(L_\star/L_\odot)$)[c]	−5.16	±	0.04
Star C Temperature[c] (K)	1130	±	50
Star C Age (Gyr)[c]	5	±	1

Notes.
[a] Inferred through *VRJHK* photometry and the Dartmouth models of Dotter et al. (2008).
[b] From M15.
[c] Dependent on the BT-Settl evolutionary models of Allard et al. (2012).

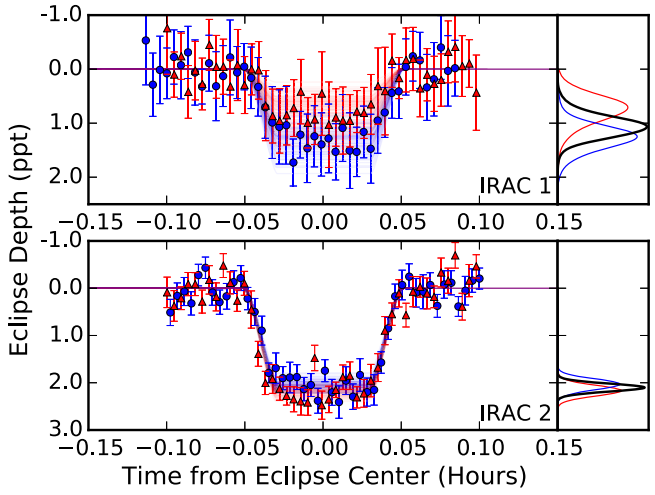

Figure 2. (Left) Observed secondary eclipses in each bandpass, with different transits in each bandpass labeled with red triangles and blue circles. A representative instrumental model has been removed for clarity. Red and blue lines represent draws from the transit model posterior distributions. (Right) Marginalized posterior distributions of the eclipse depth for each individual transit (red, blue) and combined (black). The observed eclipse depths are consistent at 1.4σ in the 3.6 μm IRAC 1 bandpass and 0.8σ in the 4.5 μm IRAC 2 bandpass. We find depths of 1.06 ± 0.21 ppt at 3.6 μm and 2.09 ± 0.08 ppt at 4.5 μm.

(2012) to infer the expected blackbody flux from the brown dwarf, finding $T_b = 1026 \pm 57$ K at 3.6 μm and $T_b = 1249 \pm 36$ K at 4.5 μm.

To test the robustness of our GP model, we calculate the maximum likelihood solutions with two different instrumental models. Following Knutson et al. (2008), we fit a second-order polynomial to the inferred centroid positions of the star to decorrelate the telescope motion from the astrophysical signal. We also apply the pixel-level decorrelation method of Deming et al. (2015), which decorates the observed fluxes against the pixel counts inside a subarray centered on the PSF of the star. In both cases, we find no statistical difference on the inferred eclipse depths.

4. TEMPERATURE AND AGE OF LHS 6343 C

Given the *Spitzer* eclipse depths and the known mass and radius of LHS 6343 C, we can infer the temperature of LHS 6343 C and the age of the system. The eclipse depths only provide a ratio between the flux from the brown dwarf and the two M dwarfs:

$$\delta = \frac{F_C}{F_A + F_B + F_C}. \quad (4)$$

We have no direct measurement of the brightness of the two M dwarfs in the IRAC bandpasses so we must infer them. M15 use the Dartmouth stellar evolutionary models of Dotter et al. (2008) to infer a mass and radius for each star given available *VRJHK* photometry. Here, we use the posterior distributions on the stellar masses and the Dartmouth models to predict the absolute magnitudes of the stars at 3.6 and 4.5 μm (Table 1). This technique also reproduces the expected brightness of the M dwarfs to within the photometric uncertainties in all bandpasses where we do have data. We then use these predictions and the observed eclipse depths to calculate the absolute magnitude of LHS 6343 C in both IRAC bandpasses: we determine $M_{C,3.6} = 13.43 \pm 0.23$ and $M_{C,4.5} = 12.58 \pm 0.07$ so that $[3.6 - 4.5] = 0.85 \pm 0.24$. We repeat this procedure with the resolved flux measurements and the BT-Settl evolutionary models of Allard et al. (2012), finding no difference in the extrapolated IRAC absolute magnitudes of the M dwarfs at the 1σ level.

Brown dwarf evolutionary models can be used to determine a temperature and age of LHS 6343 C. We investigate the predictions of several models.

The BT-Settl models provide the best fit to the available data. We use the isochrones calculated for the CIFIST 2011 abundances and opacities (Caffau et al. 2010; Allard et al. 2012), the most recent for which magnitudes have been tabulated at these masses and ages. With this model grid, we infer a brown dwarf with $t = 5 \pm 1$ Gyr, $T = 1130 \pm 50$ K, and $\log(L_\star/L_\odot = -5.16 \pm 0.04$ by evaluating the likelihood of the model fit to our calculated absolute magnitudes in each bandpass and marginalizing over all other parameters. This strategy provides an estimate of the statistical error, but not the systematic error caused by uncertainty or errors in the models. We note that of field brown dwarfs with measured temperatures and colors, this model set predicts the correct temperatures with a scatter of ~50 K, consistent with the published uncertainties in temperature.

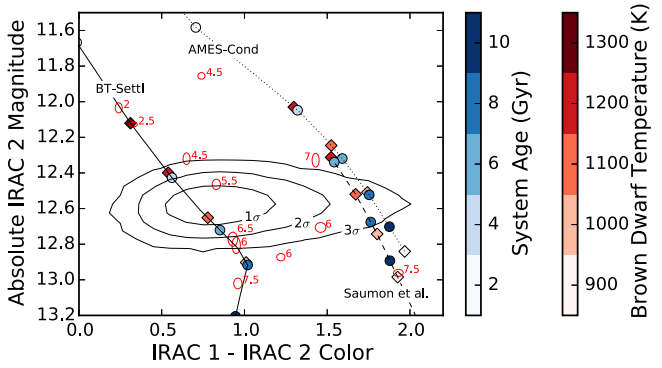

Figure 3. Color–magnitude diagram showing the absolute magnitude in the IRAC 2 4.5 μm bandpass against the IRAC 1—IRAC 2 color. Contours represent the allowed parameter space in which LHS 6343 C could reside. The labeled lines represent the theoretical evolutionary tracks of a brown dwarf with the mass of LHS 6343 C from (left to right) the BT-Settl, Saumon et al. (2012), and AMES-Cond models. Dots correspond to model predictions at (white to dark blue) 2, 4, 6, 8, and 10 Gyr; diamonds correspond to model predictions for temperatures of (white to dark red) 900, 1000, 1100, 1200, and 1300 K.The BT-Settl model provides a good fit at 5 ± 1 Gyr; the AMES-Cond and Saumon models fit the data at lower significance at 8 ± 1 Gyr. Red ellipses represent field brown dwarfs from Dupuy & Liu (2012) and Filippazzo et al. (2015); labels represent the spectral subtype inside the T class.

The AMES-Cond models of Allard et al. (2001) provide a fit to the *Spitzer* photometry, mass, and radius of LHS 6343 C such that $t = 8 \pm 1$ Gyr and $T = 1000 \pm 50$ K. However, this model grid underpredicts the 3.6 μm luminosity, leading to an overestimation of the [3.6–4.5] color at all ages (Figure 3). The AMES-Dusty models, meanwhile, do not provide a good fit, overpredicting the luminosity even if the system were the age of the universe, as is common with brown dwarf models (Rice et al. 2010; Dupuy et al. 2015).

The isochrones of Saumon & Marley (2008) combined with synthetic photometry from Saumon et al. (2012) predict IRAC photometry as a function of temperature and system age. These models provide a slightly better fit to the data than the AMES-Cond models for an 1100 ± 50 K brown dwarf, but still overpredict the [3.6–4.5] color. Their hybrid models, meant to model the L/T transition, suggest an older brown dwarf with an age of 8 ± 1 Gyr. Their cloudy L dwarf models do not provide a good fit at any age. Given the inability of the cloudy models to explain the observations, as well as the consistency between models in predicting temperatures below the L/T transition (Burgasser et al. 2002; Golimowski et al. 2004), we confirm LHS 6343 C as a T dwarf.

Objects near the L/T transition with temperatures 1000–1400 K are particularly challenging for brown dwarf evolutionary models. The uncertainties in all models are dominated by systematics, so we cannot develop one statistical posterior on the temperature or age. We note the BT-Settl models provide the best fit to these data and to the population of similar mid-T dwarfs in color–magnitude space. This system compares favorably to other known T5-6 dwarfs (Dupuy & Liu 2012, Figure 3). Of the field brown dwarfs with measured luminosities and temperatures, it is consistent with being between T4.5 dwarf 2MASS 0000 + 2554 (1227 ± 95 K) and T6 dwarfs 2MASS 0243-2453 (973 ± 83 K) and 2MASS 1346-0031 (1011 ± 86 K, Filippazzo et al. 2015) in its evolution. This age measurement, while model dependent, is the first measurement of the age of the system: previously, Johnson et al. (2011) were able to only place a lower limit of 1–2 Gyr on the system age.

5. DISCUSSION

5.1. Irradiation from LHS 6343 A

Here, we ignore irradiation from LHS 6343 A. Given the (Dartmouth model-dependent) temperature of the host of 3430 ± 20 K and semimajor axis $a/R_\star = 46.0 \pm 0.4$, the equilibrium temperature of the brown dwarf is $T_{\rm eq} = 365 \pm 3$ K, assuming a Bond albedo of 0.07, expected for a massive brown dwarf around an M2V dwarf (Marley et al. 1999). Therefore, the emitted flux as a result of the absorption and reemission of stellar radiation from LHS 6343 A is ≈1% the total flux. While irradiation may affect the thermal profile of the brown dwarf, it should be negligible considering the ≈0.1 mag uncertainties on the brown dwarf's magnitude.

Moreover, given the advanced age of the system, we expect high energy irradiation from the host star to be negligible. West et al. (2008) find a rapid decay in M dwarf magnetic activity over stellar age; Shkolnik & Barman (2014) find the same to be true for UV emission, with a steep drop in UV emission at ages above 1 Gyr. Stelzer et al. (2013) study nearby M dwarfs to find X-ray emission decays even more quickly for M dwarfs than UV emission, with a difference of three orders of magnitude between young M dwarfs in TW Hydra and old, field M dwarfs. Any high energy radiation that may have once influenced the atmosphere of LHS 6343 C has been at a low level for billions of years, allowing the brown dwarf to achieve an equilibrium representative of field brown dwarfs.

5.2. Metallicity of LHS 6343 C

M15 infer a metallicity for the two M dwarfs in the system [a/H] = 0.02 ± 0.19. If the brown dwarf formed through core accretion, it may be expected to have a higher metallicity than its host stars (Pollack et al. 1986; Podolak et al. 1988), as is the case for the planet orbiting GJ 504 (Skemer et al. 2016). Because of the low mass of the host star and likely low mass of its protoplanetary disk (Andrews et al. 2013), it is considerably more likely this brown dwarf formed like a binary star system so that the metallicity of LHS 6343 C is likely not significantly different from its host star (Desidera et al. 2004). Additional observations that infer a spectrum of LHS 6343 C can provide tests of theoretical brown dwarf spectra given the known metallicity of the system. These tests are especially important for mid/late T dwarfs, where metallicity effects can affect near-IR colors by as much as 0.3 dex (Burningham et al. 2013).

5.3. Dynamical History of LHS 6343

The secondary eclipses are centered at phase 0.5146 ± 0.0001, corresponding to times of transit 0.185 ± 0.001 days after half-phase between successive primary transits, or an eccentricity vector $e\cos\omega = 0.0229 \pm 0.0001$. This value is consistent with that inferred from RV observations and *Kepler* photometry (0.0228 ± 0.0008, M15).

The eccentricity in the LHS 6343 A-C subsystem may be primordial or the result of dynamical perturbations from star B. LHS 6343 B is presently at a sky-projected separation of ∼20 au from the A-C subsystem. Depending on the orbit of LHS 6343 B, the system may be susceptible to Kozai–Lidov oscillations (Kozai 1962; Lidov 1962). Kozai–Lidov cycles

would lead to oscillations in the orbital inclination and eccentricity of the A-C subsystem on a timescale

$$\tau \approx P_{\rm C} \frac{M_{\rm AC}}{M_{\rm B}} \left(\frac{a_{\rm AC-B}}{a_{\rm AC}} \right)^3 (1 - e_{\rm AC-B})^{3/2}, \quad (5)$$

where $P_{\rm C}$ is the orbital period of the brown dwarf, $M_{\rm AC}$ the A-C subsystem mass, $M_{\rm B}$ the perturber mass, $a_{\rm AC-B}$ and $e_{\rm AC-B}$ the orbital semimajor axis and eccentricity of star B around the AC subsystem, and $a_{\rm AC}$ the orbital semimajor axis of C around A. The two M dwarfs have similar masses. The semimajor axis $a_{\rm AC} = 0.08$ au is known, but we only know the instantaneous sky-projected separation between AC and B is ≈20 au. Taking this value as a proxy for the true semimajor axis, we find $\tau \sim 10^6 (1 - e_{\rm AC-B})^{3/2}$ years. Even for significantly larger orbits of star B and high eccentricities, the timescales for Kozai–Lidov cycles would be shorter than the $\sim 10^{10}$ year age of the system, suggesting the system may be susceptible to Kozai–Lidov oscillations given appropriate initial conditions.

The current orbit can provide clues about the dynamical history of this system. Measurement of an inclined orbit of LHS 6343 B through astrometric monitoring could provide evidence for Kozai–Lidov cycles, as would a misalignment between the spin axis of LHS 6343 A and the orbit of LHS 6343 C. While close binaries are not always neatly aligned (Albrecht et al. 2014), they often are, especially for low-mass binaries (Harding et al. 2013; Triaud et al. 2013).

We thank the referee, Adam Burgasser, for his thorough referee report which considerably improved the quality of this paper. We thank Drake Deming for providing an early draft of his 2015 paper and a version of the underlying code. We thank Sarah Ballard and Dan Foreman-Mackey for conversations about *Spitzer* data analysis and Mark Marley and Jackie Faherty for very helpful comments on an early draft of this paper which significantly improved its quality.

This work is based on observations made with the *Spitzer* Space Telescope, which is operated by the Jet Propulsion Laboratory, California Institute of Technology under a contract with NASA. Support for this work was provided by NASA through an award issued by JPL/Caltech.

B.T.M. is supported by the National Science Foundation Graduate Research Fellowship under Grant No. DGE-1144469. J.A.J. is supported by generous grants from the David and Lucile Packard Foundation and the Alfred P. Sloan Foundation.

Facility: Spitzer (IRAC).

REFERENCES

Agol, E., Cowan, N. B., Knutson, H. A., et al. 2010, ApJ, 721, 1861
Albrecht, S., Winn, J. N., Torres, G., et al. 2014, ApJ, 785, 83
Allard, F., Hauschildt, P. H., Alexander, D. R., Tamanai, A., & Schweitzer, A. 2001, ApJ, 556, 357
Allard, F., Homeier, D., & Freytag, B. 2012, RSPTA, 370, 2765
Ambikasaran, S., Foreman-Mackey, D., Greengard, L., Hogg, D. W., & O'Neil, M. 2014, arXiv:1403.6015
Andrews, S. M., Rosenfeld, K. A., Kraus, A. L., & Wilner, D. J. 2013, ApJ, 771, 129
Ballard, S., Charbonneau, D., Deming, D., et al. 2010, PASP, 122, 1341
Buenzli, E., Apai, D., Morley, C. V., et al. 2012, ApJL, 760, L31
Burgasser, A. J., Kirkpatrick, J. D., Brown, M. E., et al. 2002, ApJ, 564, 421
Burningham, B., Cardoso, C. V., Smith, L., et al. 2013, MNRAS, 433, 457
Caffau, E., Ludwig, H.-G., Bonifacio, P., et al. 2010, A&A, 514, A92
Charbonneau, D., Allen, L. E., Megeath, S. T., et al. 2005, ApJ, 626, 523
Deming, D., Knutson, H., Kammer, J., et al. 2015, ApJ, 805, 132
Desidera, S., Gratton, R. G., Scuderi, S., et al. 2004, A&A, 420, 683
Dotter, A., Chaboyer, B., Jevremović, D., et al. 2008, ApJS, 178, 89
Dupuy, T. J., & Liu, M. C. 2012, ApJS, 201, 19
Dupuy, T. J., Liu, M. C., Leggett, S. K., et al. 2015, ApJ, 805, 56
Evans, T. M., Aigrain, S., Gibson, N., et al. 2015, MNRAS, 451, 680
Faherty, J. K., Rice, E. L., Cruz, K. L., Mamajek, E. E., & Núñez, A. 2013, AJ, 145, 2
Fazio, G. G., Hora, J. L., Allen, L. E., et al. 2004, ApJS, 154, 10
Filippazzo, J. C., Rice, E. L., Faherty, J., et al. 2015, ApJ, 810, 158
Foreman-Mackey, D., Hogg, D. W., Lang, D., & Goodman, J. 2013, PASP, 125, 306
Geweke, J. 1992, in Bayesian Statistics IV, ed. J. M. Bernardo (Oxford: Clarendon), 169
Golimowski, D. A., Henry, T. J., Krist, J. E., et al. 2004, AJ, 128, 1733
Goodman, J., & Weare, J. 2010, Commun. Appl. Math. Comput. Sci., 5, 65
Harding, L. K., Hallinan, G., Konopacky, Q. M., et al. 2013, A&A, 554, A113
Helling, C., & Casewell, S. 2014, A&ARv, 22, 80
Hora, J. L., Carey, S., Surace, J., et al. 2008, PASP, 120, 1233
Johnson, J. A., Apps, K., Gazak, J. Z., et al. 2011, ApJ, 730, 79
Knutson, H. A., Charbonneau, D., Allen, L. E., Burrows, A., & Megeath, S. T. 2008, ApJ, 673, 526
Kozai, Y. 1962, AJ, 67, 591
Lidov, M. L. 1962, P&SS, 9, 719
Mace, G. N., Kirkpatrick, J. D., Cushing, M. C., et al. 2013, ApJS, 205, 6
Mandel, K., & Agol, E. 2002, ApJL, 580, L171
Marley, M. S., Gelino, C., Stephens, D., Lunine, J. I., & Freedman, R. 1999, ApJ, 513, 879
Metchev, S. A., Heinze, A., Apai, D., et al. 2015, ApJ, 799, 154
Montet, B. T., Johnson, J. A., Muirhead, P. S., et al. 2015, ApJ, 800, 134
Podolak, M., Pollack, J. B., & Reynolds, R. T. 1988, Icar, 73, 163
Pollack, J. B., Podolak, M., Bodenheimer, P., & Christofferson, B. 1986, Icar, 67, 409
Rice, E. L., Barman, T., Mclean, I. S., Prato, L., & Kirkpatrick, J. D. 2010, ApJS, 186, 63
Saumon, D., & Marley, M. S. 2008, ApJ, 689, 1327
Saumon, D., Marley, M. S., Abel, M., Frommhold, L., & Freedman, R. S. 2012, ApJ, 750, 74
Shkolnik, E. L., & Barman, T. S. 2014, AJ, 148, 64
Siverd, R. J., Beatty, T. G., Pepper, J., et al. 2012, ApJ, 761, 123
Skemer, A. J., Morley, C. V., Zimmerman, N. T., et al. 2016, ApJ, 817, 166
Stassun, K. G., Mathieu, R. D., & Valenti, J. A. 2006, Natur, 440, 311
Stelzer, B., Marino, A., Micela, G., López-Santiago, J., & Liefke, C. 2013, MNRAS, 431, 2063
Triaud, A. H. M. J., Hebb, L., Anderson, D. R., et al. 2013, A&A, 549, A18
Werner, M. W., Roellig, T. L., Low, F. J., et al. 2004, ApJS, 154, 1
West, A. A., Hawley, S. L., Bochanski, J. J., et al. 2008, AJ, 135, 785